

ERNST-MORITZ-ARNDT UNIVERSITY OF  
GREIFSWALD

MASTER THESIS

---

Kinetic effects in RF discharges

---

*Author:*  
Philipp Hacker

*Supervisor:*  
Prof. Dr. Ralf Schneider

*A thesis submitted in fulfillment of the requirements  
for the degree of Master of Science - Physics*

*in the research group of*

Computational Sciences,  
Institute of Physics



July 21, 2017

“Without encroaching upon grounds appertaining to the theologian and the philosopher, the domain of natural sciences is surely broad enough to satisfy the wildest ambition of its devotees. [...] The work may be hard, and the discipline severe; but the interest never fails, and great is the privilege of achievement. ”

— John William Strutt, 3rd Baron Rayleigh, 1884  
*in: Address to the British Association in Montreal*

# Declaration of Authorship

I hereby certify that this thesis has been composed by me and is based on my own work, unless stated otherwise. No other person's work has been used without due acknowledgement in this thesis. All references and verbatim extracts have been quoted, and iall sources of information, including graphs and data sets, have been specifically acknowledged.

.....

*Signature of author*  
Greifswald; July 21, 2017



# Contents

<b>0</b>	<b>Abstract</b>	<b>1</b>
<b>1</b>	<b>Physical properties of low temperature RF plasma</b>	<b>3</b>
1.1	Plasma physics . . . . .	3
1.1.1	Capacitively coupled radio frequency plasma . . . . .	3
1.1.2	Sheath physics and wall interaction . . . . .	4
1.1.3	Bohm criteria . . . . .	4
1.1.4	Self bias voltage . . . . .	5
1.1.5	Dielectric displacement current . . . . .	5
1.1.6	Heating mechanisms . . . . .	5
1.2	Negative ion physics . . . . .	5
1.2.1	Anion creation and distribution . . . . .	5
1.2.2	Dynamics and collisions . . . . .	5
1.3	Particle-In-Cell simulations with Monte Carlo-Colissions . . . . .	5
1.3.1	Principles . . . . .	5
1.3.2	2d3v PIC . . . . .	5
1.3.3	Monte Carlo-Collisions . . . . .	5
<b>2</b>	<b>Validation of Simulation by 1d comparison</b>	<b>7</b>
2.1	Axial density profiles . . . . .	7
2.2	Velocity and energy distributions . . . . .	7
2.3	Transition to 2d simulation . . . . .	7
<b>3</b>	<b>Simulation of capacitively coupled rf discharges</b>	<b>9</b>
3.1	Experimental setup . . . . .	9
3.2	Secondary ion emission . . . . .	9
3.3	Anion energy distributions in oxygen . . . . .	9
<b>4</b>	<b>Epilogue</b>	<b>11</b>
4.1	Local electrostatic field solver . . . . .	11
4.2	Diagnostics of current and charge . . . . .	11
4.3	Field calculation . . . . .	11
4.4	Comparison with Poisson-based solvers . . . . .	11
<b>5</b>	<b>Conclusion</b>	<b>13</b>
<b>A</b>	<b>Appendix</b>	<b>15</b>



# List of Abbreviations

abbreviation	full expression
e.g.	exempli gratia; <i>for example</i>
etc.	et cetera; <i>and so on</i>
ac	alternating current
dc	direct current
rf	radio frequency
ccrf	capacitively coupled radio frequency

**Table 1:** List of abbreviations and their corresponding phrases. If specified, the translation or an equivalent expression is written.





# Physical Quantities

Quantity	Unit	Symbol	Dimension	Value
Speed of Light	m/s	$c_0$		$2,997 \cdot 10^8$
Vacuum permittivity	F/m	$\varepsilon_0$	$s^4 A^2 m^{-3} kg^{-1}$	$8,854 \cdot 10^{-12}$
Boltzmann constant	eV/K	$k_B$	$JK^{-1}$	$8,617 \cdot 10^{-23}$
planck constant	eVs	$\hbar$	$m^2 kg s^{-1}$	$4,1345 \cdot 10^{-15} \text{ eVs}$ $6,646 \cdot 10^{-34} \text{ Js}$
particle mass	kg	$m_j$		electron: $9,109 \cdot 10^{-31}$ ion: $5,310 \cdot 10^{-26}$ anion: $5,143 \cdot 10^{-26}$
kinetic temperature	eV	$T_j$	K	$1 \text{ eV} = 1,902 \cdot 10^{-19} \text{ K}$
elementary charge	C	$e$	As	$1,902 \cdot 10^{-19}$
reduced mass	kg	$\mu_{j,k}$		$(1/m_j + 1/m_k)^{-1}$
particle density	$cm^{-3}$	$n_j$	$m^{-3}$	
Debye length	cm	$\lambda_{D,j}$	m	
plasma frequency	Hz	$\omega_{p,j}$	$s^{-1}$	
thermal velocity	m/s	$v_{th,j}$		
collisional frequency	Hz	$\nu_j$	$s^{-1}$	
particle distance	cm	$\bar{b}$	m	
mean free path	cm	$s_{mfp,j}$	m	
electrostatic potential	V	$\Phi, U$	$kg m^2 A^{-1} s^{-3}$	

**Table 2:** Physical properties in their commonly — or for this purpose most convenient — units and corresponding SI units. If not specified, the values of each quantity refer to the afore-mentioned units.



# Abstract

The Thesis Abstract is written here and usually kept to just this page. The page is kept centered vertically so it can expand into the blank space above the title too.



# Physical properties of low temperature RF plasma

In this first chapter I will provide the necessary physical background for this work about the numerical simulation of low temperature capacitively coupled radio frequency plasma. Here both the mathematical basics and method for the simulation, as well as the most important aspects about the plasma properties will be explained.

## 1.1 Plasma physics

### 1.1.1 Capacitively coupled radio frequency plasma

The experiment where after the conducted simulations is modelled after revolves around a capacitively coupled radio frequency, low temperature plasma at low pressures of oxygen.

Here, I will refer to a plasma as an globally quasi-neutral gas, consisting of freely moving charges — e.g. electrons, positively and negatively ions — and neutral gas particles. The ratio between charged and neutral species defines the *degree of ionization*, which in this case is very low. The term of global neutrality emphasizes the purpose for different length scales inside the gas itself. Hence, the associated condition of neutrality by equal densities  $n_e = n_i$  only is valid for areas larger than the so called *Debye sphere*. Inside this ball with a radius of  $\lambda_D$ , the *Debye length*, the afore-mentioned neutrality is not satisfied.

The creation of a plasma is accomplished by 2 parallel metal plates — the electrodes — where on at least one an AC signal at radio frequency is applied — this kind of experimental setup is among the most common, thus being used for basic but also in-depth studies of the afore-mentioned discharges. Here, a rf signal at exactly 13,56 MHz with an amplitude between 100–1000 V will be used — this corresponds to a wavelength of 22,11 m for the excitation. The use of external magnetic fields is not within the scope of this work — correspondingly, the experiment I will refer to also did not include  $\vec{B}$ -fields.

That said, a multitude of electric setups are possible, such as coated or grounded electrodes. Therefore, different regimes of operation ensue. For example, differently driven or shaped metal plates heavily influence the charge creation process inside the plasma. In summary, the electrodes, neutral gas and electric layout resemble a dielectric hindered plate capacitor. This simplification can be used to access important physical properties, such as an additional voltage offset on one of the electrodes or charge currents at such. A basic scheme of an asymmetric rf discharge can be seen in figure 1.1.

In the case of different electrode sizes, as seen in the scheme, the potential inside the spatially restricted area between wall and discharge can change drastically. This plasma sheath forms also between grounded parts of discharge containment or probes and plasma volume. This additional direct current offset is called *self-bias* (see section 1.1.4). A dielectric displacement current between plasma sheath and volume accommodates as a result of the different time scales of particle movement (see section 1.1.5). Especially, self-bias and displacement current play a key role in the following investigations, as a capacitive coupling between electrodes and power supply is difficult to model into a numerical kinetic simulation.

In comparison to other low temperature, low pressure discharges — an example could be a dielectric hindered dc discharge at high voltages, with an electrode space gap of just a couple millimeters —, radio frequency plasma are characterized by their unique transport process inside the sheath and heating mechanisms of charged species. A more in-depth discussion can be found in section 1.1.6.

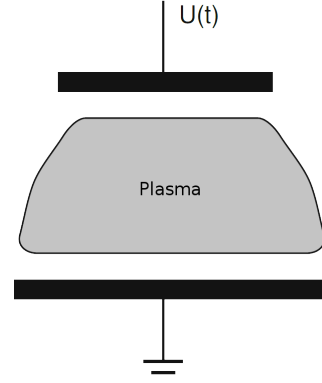


**Figure 1.1:** Schematic of an asymmetric discharge with one grounded and one driven electrode. The rf signal is denoted with  $U(t)$ .

## 1.1.2 Sheath physics and wall interaction

### 1.1.3 Bohm criteria

In section 1.1.2 the behaviour of charge particle densities inside the plasma sheath has been discussed. In contrast to the discharge volume, those densities do not satisfy the quasi-neutrality condition in a distance of  $d$  from the wall anymore. Though we know that the sheath is a spatially restricted area around electrostatic floating surfaces, a physical law concerning this circumstance has not been derived here. So the question ensues, why the area of electron depletion does not extend further into the discharge volume.

To answer this question, one has to take a look at substitutional system. This will be a, likewise mechanical, one-body extremal problem of a point mass. In this case only kinematic potentials with inverted parabolic maxima are of interest. Therefore, in this unstable equilibrium a small perturbation culminates into a large force on the test body.

To see the quality of this example, one has to take a look at the second order differential equation of the afore-mentioned mechanical problem and the electrostatic *Poisson's equation* (see equation 1.1).

$$m \frac{d^2 \vec{r}}{dt^2} = - \frac{dV}{d\vec{r}} \quad \Leftrightarrow \quad \Delta_{\vec{r}} \Phi = - \frac{d\Psi}{d\Phi} = f(\Phi) \stackrel{\text{Poisson's}}{=} \frac{\rho}{\epsilon_0} \quad (1.1)$$

For an instability, the force on the test body must increase with the distance from the equilibrium, hence the equation 1.3 is used to calculate the exact velocity at which an ion is entering the sheath. This results in the first *Bohm criteria*.

$$0 > \left. \frac{d^2\Psi}{d\Phi^2} \right|_{\Phi=0} \stackrel{\text{equation 1.1}}{=} \left. \frac{d}{d\Phi} \left( \frac{n_e(x) - n_i(x)}{\varepsilon_0} \right) \right|_{\Phi=0} = \frac{en_e(-d)}{\varepsilon_0} \left( \frac{e}{k_b T_e} - \frac{e}{m_i v_{i,0}^2} \right) \quad (1.2)$$

$$\Rightarrow v_{i,0} \geq v_{B,i} = \sqrt{\frac{k_B T_e}{m_i}} \quad (1.3)$$

#### 1.1.4 Self bias voltage

#### 1.1.5 Dielectric displacement current

#### 1.1.6 Heating mechanisms

### 1.2 Negative ion physics

#### 1.2.1 Anion creation and distribution

#### 1.2.2 Dynamics and collisions

### 1.3 Particle-In-Cell simulations with Monte Carlo-Colissions

#### 1.3.1 Principles

#### 1.3.2 2d3v PIC

#### 1.3.3 Monte Carlo-Collisions





# Validation of Simulation by 1d comparison

2.1 Axial density profiles

2.2 Velocity and energy distributions

2.3 Transition to 2d simulation



# Simulation of capacitively coupled rf discharges

3.1 Experimental setup

3.2 Secondary ion emission

3.3 Anion energy distributions in oxygen



# Epilogue

- 4.1 Local electrostatic field solver
- 4.2 Diagnostics of current and charge
- 4.3 Field calculation
- 4.4 Comparison with Poisson-based solvers



## Conclusion





# Appendix

quantity	equation	relevance
Debye length	$\lambda_{D,j}^2 = \frac{\varepsilon_0 k_B T_j}{n_j e^2}$ $\lambda_D^2 = \left( \lambda_{D,e}^{-2} + \lambda_{D,i}^{-2} \right)^{-1}$	distance around a charge, at which quasi-neutrality is satisfied, $\lambda_D$ is the combined screening length from individual species
plasma parameter	$N_D = n \frac{4}{3} \pi \lambda_D^3$	number of particles inside Debye sphere, if $N_D \gg 1$ an ionized gas is considered a plasma (degree of ionization)
plasma frequency	$\omega_{p,j}^2 = \frac{n_j e^2}{\varepsilon_0 m_j} = \frac{v_{th,j}}{\lambda_{D,j}} = \frac{1}{\tau_j}$	upper limit for interaction with fields/forces or external excitations inverse screening time
thermal velocity	$v_{th,j}^2 = \frac{k_B T_j}{m_j}$	mean velocity from kinetic theory of gases
coulomb logarithm	$\ln(\Lambda)$ $\Lambda = \frac{b_{\max}}{b_{\min}} = \lambda_D \cdot \frac{4\pi\varepsilon_0 \mu v_{th}^2}{e^2}$	dimensionless scale for transport processes inside discharge fraction of probability for a cumulative 90° scattering by many small perturbation collisions and a single right angle scattering
collision frequency	$\nu_j = \frac{e^4 n_j \ln(\Lambda)}{8\sqrt{2} m_j \pi \varepsilon_0 (k_B T_j)^{3/2}}$	two body coulomb collision frequency inside species j
particle distance & mean free path	$\bar{b} = \frac{\hbar}{m_j v_{th,j}}$ $s_{mfp,j} = \frac{v_{th,j}}{\nu_{j,k}}$	mean inter particle distance for species j free flight between subsequent collisions of species j and k with collision frequency $\nu_{j,k}$

quantity	equation	relevance
speed of sound	$c_S^2 = \frac{\gamma Z k_B T_e}{m_i}$	speed of longitudinal ion waves at electron pressure
	$\gamma = 1 + 2/f = 5/3$	adiabatic coefficient with f, the kinetic degree of freedom
Debye-Hückel potential	$\Phi = \frac{Q}{4\pi\epsilon \vec{r} } e^{-\frac{ \vec{r} }{\lambda_D}}$	electrostatic potential of charge particle $Q$ at distance $ \vec{r} $ equal to coulomb interaction with additional shielding by charged particles

**Table A.1:** Selection of physical properties of a low temperature ccrf discharge. The index  $j$  denotes the species, e.g. electrons, ions. Used quantities can be found in the preface in table 2.